Mesoporous Materials

DOI: 10.1002/ange.201402214

Responsive Mesoporous Photonic Cellulose Films by Supramolecular Cotemplating**

Michael Giese, Lina K. Blusch, Mostofa K. Khan, Wadood Y. Hamad, and Mark J. MacLachlan**

Abstract: *Cellulose-based materials have been and continue to be exceptionally important for humankind. Considering the bioavailability and societal relevance of cellulose, turning this renewable resource into an active material is a vital step towards sustainability. Herein we report a new form of cellulose-derived material that combines tunable photonic properties with a unique mesoporous structure resulting from a new supramolecular cotemplating method. A composite of cellulose nanocrystals and a urea–formaldehyde resin organizes into a chiral nematic assembly, which yields a chiral nematic mesoporous continuum of desulfated cellulose nanocrystals after alkaline treatment. The mesoporous photonic cellulose (MPC) films undergo rapid and reversible changes in color upon swelling, and can be used for pressure sensing. These new active mesoporous cellulosic materials have potential applications in biosensing, optics, functional membranes, chiral separation, and tissue engineering.*

Cellulose-derived products (e.g., paper) are certainly widespread and important, but they are still primarily used for low-tech applications, such as banknotes, communication, information storage, packaging, and construction.[1] There is growing interest in applying cellulose to advanced technologies, as it is a widely available, renewable resource. Recently, cellulosic materials functionalized with additives have been demonstrated for sensing,[2] magnetism,[3] and catalysis;[4] however, in these roles, cellulose continues to merely serve as a passive substrate for the functional component. A cellulose material with an ordered mesoporous structure is attractive for the development of new applications, but liquid-crystal templating strategies previously applied to the construction of mesoporous silicates and other materials have not been applied to cellulose.[5]

Cellulose nanocrystals (CNCs)[6] are obtained by the treatment of cellulosic biomass with sulfuric acid, which leads to sulfate ester groups on the surface of the CNCs.[7] These charges are relevant both for stabilizing colloidal suspensions of the CNCs and for enabling them to form a chiral nematic liquid-crystalline phase in water.[8] Following the evaporation of water, CNCs retain their chiral nematic order as they self-assemble into iridescent films.[9] The photonic properties of these films are of interest for coloration, reflectors, and security features.[10] The dense films can be swollen with water vapor and thus function as a humidity sensor;[11] however, one significant problem is that the sulfated CNCs are inherently susceptible to redissolution in water. A chiral nematic structure of unfunctionalized CNCs would be more stable, but desulfated CNCs are not known to assemble into chiral nematic structures.[6b] Interestingly, partial desulfation of preassembled CNC films by thermal treatment was previously shown to make the films less susceptible to redispersion in water.[10c,12]

One way to stabilize the chiral nematic structure of CNCs is to polymerize suitable monomers in the presence of the ordered lyotropic liquid crystal. It was recently demonstrated that the chiral nematic structure of CNCs could be captured in silica/CNC,[13] hydrogel/CNC,[14] amino–formaldehyde/CNC,[15] and phenol–formaldehyde/CNC[16] composites.

In this study, the chiral nematic structure of CNCs was preserved in a two-step synthesis to yield mesoporous photonic cellulose (MPC) films (Figure 1). In the first step, chiral nematic composite films (CNC-UF) were synthesized by the self-assembly of lyotropic CNCs in the presence of a urea formaldehyde (UF) precursor (see Figure S1 in the Supporting Information). The CNC/UF mixture was dried overnight under ambient conditions, followed by heat curing at 120 °C to complete the polymerization. Various CNC-UF composite materials were synthesized either by changing the polymer/CNC ratio (CNC-UF-A) or by the addition of salts (CNC-UF-B; see the Supporting Information for details). These composite materials provide the basis for a range of MPCs with different optical properties. However, to maximize the structural flexibility and mesoporosity of the films, we used samples with a high content of the UF precursor (CNC-UF-A4).

In the second step, alkaline treatment of the composite films with 15% aqueous KOH at 70 °C removed the UF and resulted in iridescent and insoluble cellulose films (MPC). This method is a novel approach towards the creation of

[*] Dr. M. Giese, Dr. L. K. Blusch, Dr. M. K. Khan, Prof. M. J. MacLachlan
Department of Chemistry, University of British Columbia
2036 Main Mall, Vancouver, BC, V6T 1Z1 (Canada)
E-mail: mmaclach@chem.ubc.ca
Homepage: http://www.chem.ubc.ca/mark-maclachlan
Dr. W. Y. Hamad
FPInnovations
3800 Wesbrook Mall, Vancouver, BC, V6S 2L9 (Canada)
E-mail: wadood.hamad@fpinnovations.ca

[**] Financial support from ArboraNano, NSERC, NORAM Engineering and Constructors Ltd., the German Academic Exchange Service (DAAD) (fellowship to M.G.), and the Humboldt Foundation (fellowship to L.K.B.) is gratefully acknowledged. We appreciate the in-kind contribution of CNCs from FPInnovations and CelluForce Inc. We thank A. Lam, J. Drummond, and J. A. Kelly for experimental assistance.

Supporting information for this article is available on the WWW under http://dx.doi.org/10.1002/anie.201402214.

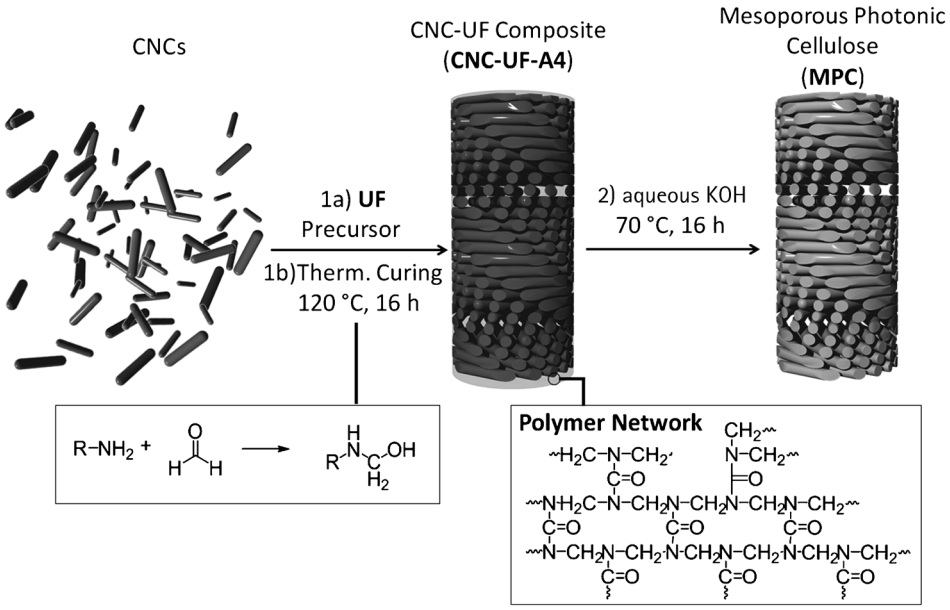

Figure 1. Synthetic route to mesoporous photonic cellulose (MPC). An aqueous suspension of CNCs is combined with a UF precursor. Following evaporation-induced self-assembly, a CNC-UF composite (CNC-UF-A4) with chiral nematic order is obtained. Thermal curing of the composite is followed by treatment with aqueous KOH to yield MPC.

cellulosic materials by supramolecular cotemplating, whereby UF and CNCs act as synergetic templates. The simple strategy leads to a functional cellulose film with chiral nematic order, enhanced stability, flexibility, and mesoporosity.

In fact, we expected that alkaline treatment in the second step would simply destroy the CNC template to leave a mesoporous UF resin, since similar conditions were previously used to remove CNCs from phenol–formaldehyde/CNC composites.[16] Most interestingly, however, elemental analysis of the product showed no nitrogen! This result indicated the decomposition of the UF resin, as further supported by the disappearance of the diagnostic carbonyl C=O stretching vibration found at 1664 cm^{-1} for CNC-UF composites (see Figure S2). Moreover, the solid-state ^{13}C cross-polarization/magic-angle-spinning (CP/MAS) NMR spectrum of MPC showed significant changes with respect to that of the composite (Figure 2a). Whereas the carbonyl and methylene signals assigned to the UF resin are clearly present in the ^{13}C NMR spectrum of the composites, they vanished in the spectrum of MPC. Furthermore, the solid-state ^{13}C CP/MAS NMR spectrum of MPC showed all expected peaks for crystalline cellulose I. However, signal broadening as well as new peaks at approximately 84 and 62 ppm assigned to amorphous or surface cellulose (C4′ and C6′, respectively) proved significant loss of crystallinity.[17] We believe that the relative stability of the CNCs under the caustic conditions can be attributed to the fact that the CNCs are embedded in the UF polymer network, which degrades first and protects the CNCs.[18]

In line with solid-state ^{13}C CP/MAS NMR spectroscopy, powder X-ray diffraction (PXRD) patterns indicated that the MPC films have a substantially lower degree of crystallinity (ca. 70%) than that of pure CNCs (> 90%), but maintain the natural cellulose I structure (Figure 2b; see also Figures S3 and S4). Notably, a control experiment in which pristine CNCs were treated with 15% aqueous KOH under identical conditions led to mercerization of the cellulose (conversion of cellulose I into cellulose II; see Figure S3b).[19]

Nitrogen-adsorption measurements indicated that chiral nematic CNC films and CNC-UF composites are both nonporous, as are MPC films dried under ambient conditions from water or ethanol. However, ethanol-soaked MPC samples dried from supercritical CO_2 showed significant mesoporosity. Thus, effective removal of the space-filling UF cotemplate produces mesopores between the cellulose nanocrystals. This experimental finding is novel. Films from which water had been removed by drying showed a significant surface area after reswelling in EtOH and subsequent supercritical drying. Moreover, N_2 adsorption showed a type IV isotherm with a Brunauer–Emmett–Teller (BET) surface area as high as 252 $m^2 g^{-1}$ and an average pore volume of 0.6 $cm^3 g^{-1}$ (Figure 2c). The calculated Barrett–Joyner–Halenda (BJH) pore-size distribution had a peak at about 8 nm (Figure 2c, inset).

In contrast to regular CNC films, however, which disperse in 1–2 h in water, MPC was stable in water for weeks, and even boiling did not result in any decomposition. The enhanced stability of the MPC in water arises from desulfation of the CNC surface. Indeed, there was no detectable sulfur present in MPC samples, thus indicating that all of the sulfate groups were removed (see the Supporting Information). Desulfation, which results from the supramolecular cotemplating process, leads to uncharged photonic MPC films that are not dispersible in water. As already mentioned, desulfated CNCs do not naturally self-assemble into a chiral nematic structure; the supramolecular cotemplating approach, however, allows one to obtain, in a novel way, a desulfated CNC material with the chiral nematic structure preserved. It is thought that the chiral nematic structure is preserved as a result of concomitant desulfation and destruction of the UF resin. Furthermore, it is reasonable to expect that some of the surface hydroxy groups of the CNCs may be cross-linked by the excess formaldehyde to form methylene ether bridges, as this reaction is widely known for cellulose.[20] We did not detect such methylene bridges by spectroscopy or analysis, so their concentration is probably negligible.

On the basis of detailed IR and solid-state NMR spectroscopy, CHNS analysis, gas adsorption, and PXRD data, it is evident that MPC is made of cellulose I (exactly the same form as that for the starting CNC material). MPC films

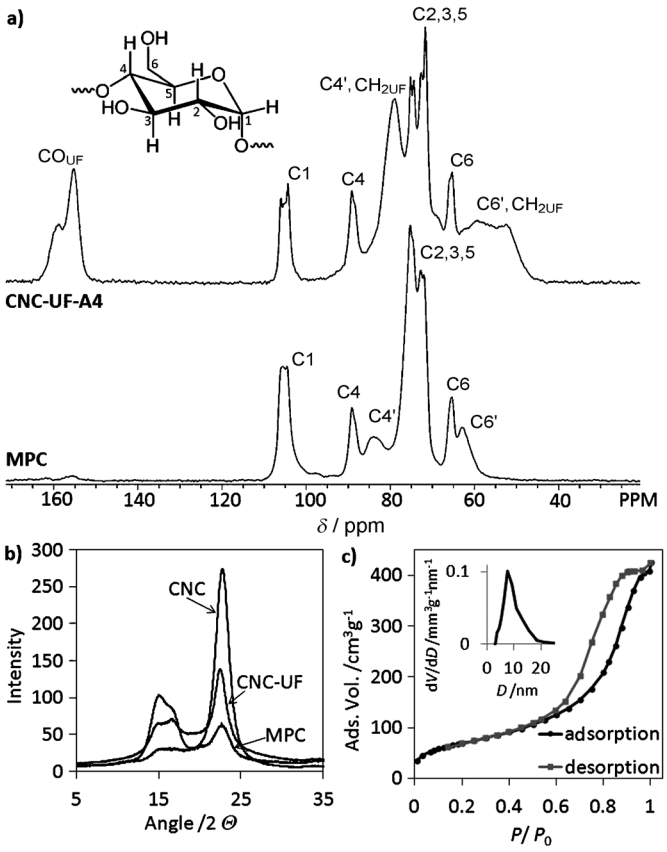

Figure 2. Structural characterization of the MPC. a) Solid-state ^{13}C CP/MAS NMR spectra of the composite CNC-UF-A4 and MPC. b) PXRD pattern of pristine CNCs (cellulose I), the CNC-UF-A4 composite, and MPC. c) Isothermal N_2 adsorption of MPC dried from EtOH with supercritical CO_2 (BET surface area), as well as the corresponding BJH pore-size distribution calculated from the adsorption branch of the isotherm (inset).

showed similar thermal stability (see Figure S5) to that of sodium salts of CNCs and the CNC-UF composite films. In terms of the characteristic mechanical behavior, highly flexible MPC films have an ultimate tensile strength of (42 ± 5) MPa (see Figure S6), which is substantially higher than the tensile strength reported for graphene paper (8.8 MPa) or graphene/polyaniline paper (12.6 MPa).[21]

Retention of the chiral nematic structure in the composite and MPC films was deduced by a combination of polarized optical microscopy (POM; see Figure S7), UV/Vis spectroscopy, circular dichroism (CD) spectroscopy, and scanning electron microscopy (SEM). In general, chiral nematic structures reflect light with a wavelength (λ_{max}) that depends on the helical pitch (P), the angle of incident light (θ), and the average refractive index (n_{avg}) of the material, according to the following equation:[9,22]

$$\lambda_{max} = n_{avg} P \sin(\theta) \quad (1)$$

Thus, the color reflected by a chiral nematic structure may be modulated by manipulating the pitch or the refractive index. With increasing polymer content in CNC-UF-A1–4, a red shift was observed, whereas salt addition caused a blue shift with increasing ionic strength (CNC-UF-B1–4). Coloration of the films could be varied in the range 500 to 1300 nm (see the Supporting Information for details).

The composite CNC-UF-A4 provided an ideal basis for flexible and mesoporous MPC and appeared nearly transparent and colorless (reflecting at 1300 nm; Figure 3a; see also Figure S9). However, after removal of the cotemplating UF, the resulting MPC films dried from water showed a significant blue shift with a peak reflectance at 330 nm in the UV/Vis spectrum (Figure 3b; see also Figure S9). In contrast, MPC films dried with supercritical CO_2 were visibly iridescent, and UV/Vis spectroscopy showed that they reflected light at approximately 500 nm (Figure 3c; see also Figure S9). The red-shifted reflectance as compared to that of the water-dried samples indicates that the pitch, P, of the chiral nematic structure increases with the introduction of mesoporosity. The translucent appearance of the films is also indicative of their underlying mesoporous structure. SEM images of CNC-UF-A4, water-dried MPC, and supercritical CO_2-dried MPC all show a layered structure that is characteristic of a chiral nematic order (Figure 3a–c, bottom images). The microstructure of MPC after supercritical drying seems less ordered than that of the other samples, and this heterogeneity may contribute to the opacity of this sample.

In short, the results presented so far prove the cellulosic nature of the MPC as well as its high mesoporosity and flexibility. Owing to these properties and their chiral nematic order, the MPC materials might be useful for applications in gas separation, membranes, drug delivery, photonics, and sensing. To investigate the sensing performance of the CNC composites and the resulting MPC films, we studied swelling behavior in different polar solvents. Whereas CNC-UF composites took several hours to swell in water, reaching equilibrium after about 12 h (see Figure S10), MPC films showed a rapid red shift of their reflection peak from 330 nm for the dry film to 820 nm when immersed in polar solvents (Figure 4a–c). This response is easily observable by the naked eye and is significantly faster than those previously reported for hydrogel materials.[14a,16] It is especially remarkable considering the simplicity of the synthesized material. The degree of swelling was very sensitive to the solvent, and by varying the solvent mixture (ethanol/water), the vibrantly visible colors could be tuned from 430 nm in pure ethanol to 840 nm in pure water (Figure 4a,b). Owing to the hydrophilicity and the mesoporosity of these cellulose films, they rapidly swell to the greatest extent in pure water, which complicates the analysis of contact-angle measurements (see Figure S11). As ethanol and water have similar refractive indices, the color change is mainly attributed to a change in the helical pitch upon swelling. This change is detectable by either UV/Vis or CD spectroscopy, which may enable the development of new sensors.

To our surprise, the water-soaked MPC samples showed high flexibility and piezochromic behavior. To investigate their ability to sense pressure, we inserted water-soaked MPC films between two glass slides and followed the distinctive color change upon manually pressing the films. The macroscopically applied pressure is transferred to the nanoscale level and leads to a compression of the layers. Thus, the helical

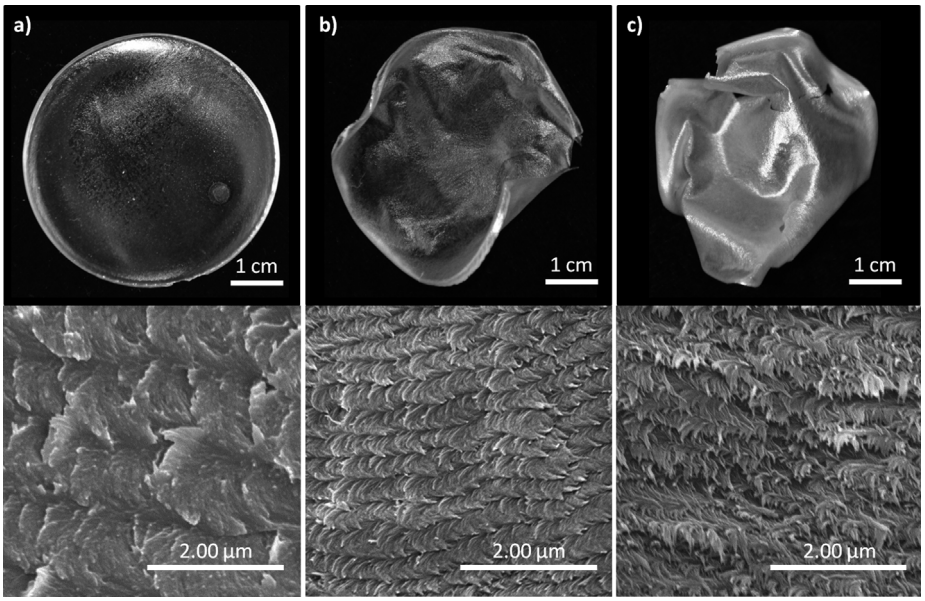

Figure 3. Optical characterization of the CNC-UF composite and the resulting MPC film. a) Photograph (top) and SEM image (bottom) of the composite film CNC-UF-A4 after curing. b) Photograph (top) and SEM image (bottom) of MPC air-dried from H_2O. c) Photograph (top) and SEM image (bottom) of MPC dried from EtOH with supercritical CO_2.

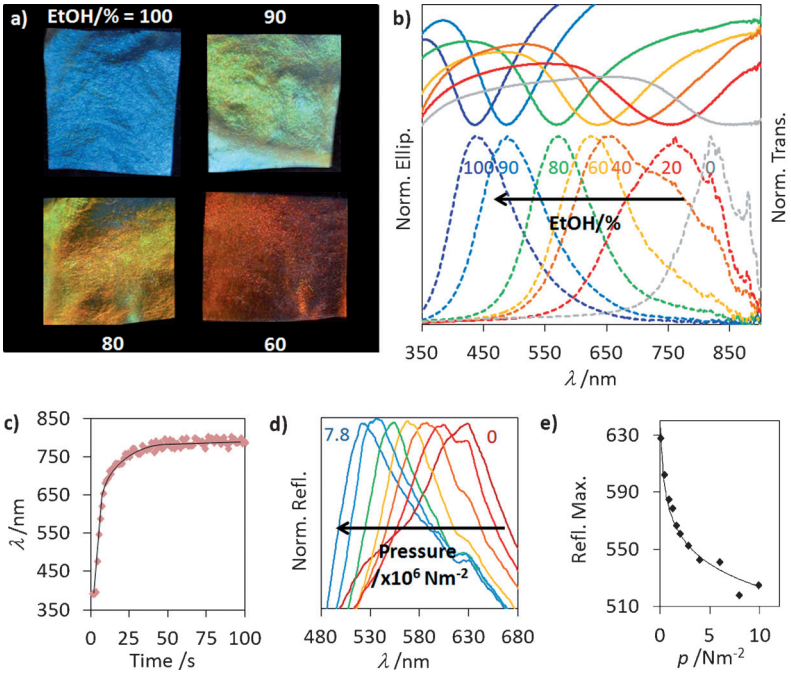

Figure 4. Sensing performance of the functional MPC films. a) Photographs and b) UV/Vis (solid lines) and CD spectra (dashed lines) of MPC soaked in EtOH/H_2O at different ratios as indicated. c) Swelling kinetics of MPC: Curve shows the dependence of the wavelengths on time when a dry sample is immersed in water. d) Pressure response of MPC at 0, 0.4, 0.8, 1.6, 2.7, 5.9, and 7.8×10^6 N m^{-2} (first and final value given in graphic) showing a clear blue shift of the peak reflectance wavelengths. e) Plot of peak reflection wavelength versus pressure. The data were fit with an exponential curve.

pitch of the chiral nematic structure is reduced. The blue shift was observed in a reflectivity range of about 100 nm, from 630 to 520 nm (Figure 4d). We quantified the change in photonic color as a function of applied pressure (Figure 4e). The coloration is completely reversible: After the applied stress is removed, the material relaxes and returns to its initial colorless state.

In summary, we have developed a new supramolecular cotemplating method in which two components function as synergetic templates. This approach has allowed us to prepare a novel mesoporous chiral cellulose material (MPC) that displays dynamic photonic properties. Owing to reduced crystallinity (relative to that of the starting CNC material), and the formation of a mesoporous structure after supercritical drying, the synthesized cellulosic films show high flexibility and conformability. These characteristics lead to rapid responses to external stimuli, such as pressure and solvent polarity. MPC is a new functional mesoporous material that is promising for new dynamically controlled optical filters and sensors. Furthermore, with its high surface area and chiral structure, MPC might be used as a functional membrane or as a hard template to access diverse mesoporous materials.

Experimental Section

Synthesis of the UF precursor: A mixture of urea (2 g, 67 mmol) and formaldehyde (10 g of a 37% solution in H_2O stabilized with 10–15% MeOH) was stirred until complete solvation. One drop of an HCl solution (37% in H_2O) was added, and the resulting opaque polymer precursor solution was heated at 100°C for 30 min until it became clear. This solution was used as the UF precursor solution.

Synthesis of MPC: The UF precursor solution (1 mL) was added to a suspension of CNCs in water (5 mL; CNC-Na, pH 6.9, 3 wt%), and the resulting mixture was stirred for 10 min at room temperature. The mixture was then transferred to a cellulose acetate surface (diameter: 5 cm) and allowed to dry for 48 h under ambient conditions. Polymerization was finalized by curing at 120°C for 16 h in an oven to give CNC-UF-A4. Following treatment with an aqueous solution of KOH (15%) at 70°C for 16 h to remove the UF, the mixture was washed with water and then with ethanol. Drying of the mixture under ambient conditions gave MPC. Mesoporous MPC was obtained by drying ethanol-soaked films with supercritical CO_2.

Received: February 8, 2014
Revised: May 14, 2014
Published online: June 30, 2014

Keywords: cellulose · color tuning · liquid crystals · mesoporous materials · photonic materials

[1] L. Febvre, H.-J. Martin, *The Coming of the Book*, Verso, London, **1976**.
[2] a) J. P. Metters, S. M. Houssein, D. K. Kampouris, C. E. Banks, *Anal. Methods* **2013**, *5*, 103 – 110; b) M. Novell, M. Parrilla, G. A. Crespo, F. X. Rius, F. J. Andrade, *Anal. Chem.* **2012**, *84*, 4695 – 4702; c) D. D. Liana, B. Raguse, J. J. Gooding, E. Chow, *Sensors* **2012**, *12*, 11505 – 11526.
[3] a) D. Fragouli, I. S. Bayer, R. Di Corato, R. Brescia, G. Bertoni, C. Innocenti, D. Gatteschi, T. Pellegrino, R. Cingolani, A. Athanassiou, *J. Mater. Chem.* **2012**, *22*, 1662 – 1666; b) R. T. Olsson, M. A. S. A. Samir, G. Salazar-Alvarez, L. Belova, V. Ström, L. A. Berglund, O. Ikkala, J. Nogués, U. W. Gedde, *Nat. Nanotechnol.* **2010**, *5*, 584 – 588.
[4] R. Bendi, T. Imae, *RSC Adv.* **2013**, *3*, 16279 – 16282.
[5] a) C. T. Kresge, M. E. Leonowicz, W. J. Roth, J. C. Vartuli, J. S. Beck, *Nature* **1992**, *359*, 710 – 712; b) G. S. Attard, J. C. Glyde, C. G. Goltner, *Nature* **1995**, *378*, 366 – 368; c) J.-S. Yang, T. M. Swager, *J. Am. Chem. Soc.* **1998**, *120*, 5321 – 5322; d) S. Inagaki, S. Guan, T. Ohsuna, O. Terasaki, *Nature* **2002**, *416*, 304 – 307; e) G. S. Armatas, M. G. Kanatzidis, *Science* **2006**, *313*, 817 – 820.
[6] a) D. Klemm, F. Kramer, S. Moritz, T. Lindström, M. Ankerfors, D. Gray, A. Dorris, *Angew. Chem.* **2011**, *123*, 5550 – 5580; *Angew. Chem. Int. Ed.* **2011**, *50*, 5438 – 5466; b) Y. Habibi, L. A. Lucia, O. J. Rojas, *Chem. Rev.* **2010**, *110*, 3479 – 3500; c) A. Dufresne, *Nanocellulose: From Nature to High Performance Tailored Materials*, Walter de Gruyter, Göttingen, **2012**; d) J. R. Capadona, K. Shanmuganathan, D. J. Tyler, S. J. Rowan, C. Weder, *Science* **2008**, *319*, 1370 – 1374; e) S. J. Eichhorn, A. Dufresne, M. Aranguren, N. E. Marcovich, J. R. Capadona, S. J. Rowan, C. Weder, W. Thielemans, M. Roman, S. Renneckar, W. Gindl, S. Veigel, J. Keckes, H. Yano, K. Abe, M. Nogi, A. N. Nakagaito, A. Mangalam, J. Simonsen, A. S. Benight, A. Bismarck, L. A. Berglund, T. Peijs, *J. Mater. Sci.* **2010**, *45*, 1 – 33; f) W. Y. Hamad, T. Q. Hu, *Can. J. Chem. Eng.* **2010**, *88*, 392 – 402.
[7] B. G. Rånby, *Discuss. Faraday Soc.* **1951**, *11*, 158 – 164.
[8] a) R. H. Marchessault, F. F. Morehead, N. M. Walter, *Nature* **1959**, *184*, 632 – 633; b) J. F. Revol, H. Bradford, J. Giasson, R. H. Marchessault, D. G. Gray, *Int. J. Biol. Macromol.* **1992**, *14*, 170 – 172.
[9] J.-F. Revol, L. Godbout, D. G. Gray, *J. Pulp Pap. Sci.* **1998**, *24*, 146 – 149.
[10] a) S. N. Fernandes, Y. Geng, S. Vignolini, B. J. Glover, A. C. Trindade, J. P. Canejo, P. L. Almeida, P. Brogueira, M. H. Godinho, *Macromol. Chem. Phys.* **2013**, *214*, 25 – 32; b) Y. P. Zhang, V. P. Chodavarapu, A. G. Kirk, M. P. Andrews, *J. Nanophoton.* **2012**, *6*, 063516 – 063519; c) D. L. Godbout, D. G. Gray, J. F. Revol (Pulp and Paper Research Institute of Canada), EP0745112 B1, **1995**; d) C. Edgar, D. Gray, *Cellulose* **2001**, *8*, 5 – 12; e) S. Beck, J. Bouchard, G. Chauve, R. Berry, *Cellulose* **2013**, *20*, 1401 – 1411; f) M. S. Vlad-Cristea, V. Landry, P. Blanchet, C. Ouellet-Plamondon, *ISRN Nanomaterials* **2013**, *2013*, 1 – 12; g) A. Querejeta-Fernández, G. Chauve, M. Methot, J. Bouchard, E. Kumacheva, *J. Am. Chem. Soc.* **2014**, *136*, 4788 – 4793.
[11] Y. P. Zhang, V. P. Chodavarapu, A. G. Kirk, M. P. Andrews, *Sens. Actuators B* **2013**, *176*, 692 – 697.
[12] F. Jiang, A. R. Esker, M. Roman, *Langmuir* **2010**, *26*, 17919 – 17925.
[13] K. E. Shopsowitz, H. Qi, W. Y. Hamad, M. J. MacLachlan, *Nature* **2010**, *468*, 422 – 425.
[14] a) J. A. Kelly, A. M. Shukaliak, C. C. Y. Cheung, K. E. Shopsowitz, W. Y. Hamad, M. J. MacLachlan, *Angew. Chem.* **2013**, *125*, 9080 – 9084; *Angew. Chem. Int. Ed.* **2013**, *52*, 8912 – 8916; b) J. Zoppe, L. Grosset, J. Seppälä, *Cellulose* **2013**, *20*, 2569 – 2582.
[15] M. Giese, M. K. Khan, W. Y. Hamad, M. J. MacLachlan, *ACS Macro Lett.* **2013**, *2*, 818 – 821.
[16] M. K. Khan, M. Giese, M. Yu, J. A. Kelly, W. Y. Hamad, M. J. MacLachlan, *Angew. Chem.* **2013**, *125*, 9089 – 9092; *Angew. Chem. Int. Ed.* **2013**, *52*, 8921 – 8924.
[17] C. H. Lemke, R. Y. Dong, C. A. Michal, W. Y. Hamad, *Cellulose* **2012**, *19*, 1619 – 1629.
[18] a) J. Dutkiewicz, *J. Appl. Polym. Sci.* **1983**, *28*, 3313 – 3320; b) I. S. Chuang, G. E. Maciel, *Macromolecules* **1992**, *25*, 3204 – 3226.
[19] D. Klemm, B. Heublein, H.-P. Fink, A. Bohn, *Angew. Chem.* **2005**, *117*, 3422 – 3458; *Angew. Chem. Int. Ed.* **2005**, *44*, 3358 – 3393.
[20] a) M. Schenk, *Helv. Chim. Acta* **1931**, *14*, 520 – 541; b) E. J. Blanchard, R. M. Reinhardt, E. E. Graves, B. A. K. Andrews, *Ind. Eng. Chem. Res.* **1994**, *33*, 1030 – 1034; c) B. Singh, C. L. Jain, A. Pande, V. B. Chipalkatti, R. S. Parikh, *Text. Res. J.* **1970**, *40*, 940 – 947; d) S. P. Rowland, M. L. Rollins, I. V. Degruy, *J. Appl. Polym. Sci.* **1966**, *10*, 1763 – 1776.
[21] D.-W. Wang, F. Li, J. Zhao, W. Ren, Z.-G. Chen, J. Tan, Z.-S. Wu, I. Gentle, G. Q. Lu, H.-M. Cheng, *ACS Nano* **2009**, *3*, 1745 – 1752.
[22] H. De Vries, *Acta Crystallogr.* **1951**, *4*, 219 – 226.

